Informes Técnicos Ciemat **1470**

Ju Oio, 2020

EVOLUTION OF THE ROTATIONAL TRANSFORM IN TJ-II DISCHARGES USING THE ASTRA CODE

D. López Bruna[1]
J.M. Reynolds-Barredo[2]
B. Momo[3]

(1) CIEMAT
(2) Universidad Carlos III
(3) Consorzio RFX

Laboratorio Nacional de Fusión

Publication available in catalog of official publications

ISSN:
NIPO:832-20-004-X

Edition and Publication:
Editorial CIEMAT
Avda. Complutense, 40 28040-MADRID
e-mail: editorial@ciemat.es
Editorial news

EVOLUCIÓN DE LA TRANSFORMADA ROTACIONAL EN DESCARGAS DEL TJ-II USANDO EL SISTEMA ASTRA

D. López Bruna, J.M. Reynolds-Barredo, B. Momo

28 pp, 19 refs., 6 figs., 1 tbls.

Resumen:

En un trabajo previo [Informes Técnicos Ciemat 1201, CIEMAT, Marzo 2010] se extendió el sistema ASTRA [Tech. Rep. IPP 5/98, Max Plank Institut für Plasmaphysik, Garching, February 2002] añadiendo varios códigos periféricos que aumentan las capacidades de cálculo de transporte para los plasmas de la instalación TJ-II (Laboratorio Nacional de Fusión, CIEMAT). Poco después se incluyeron los cálculos de equilibrio y de la evolución de la transformada rotacional, los cuales documentamos aquí informando además sobre los métodos de cálculo y dando una pequeña guía de usuario.

EVOLUTION OF THE ROTATIONAL TRANSFORM IN TJ-II DISCHARGES USING THE ASTRA SHELL.

D. López Bruna, J.M. Reynolds-Barredo, B. Momo

28 pp, 19 refs., 6 figs., 1 tbls.

Abstract:

In a previous work [Informes Técnicos Ciemat 1201, CIEMAT, March 2010], the Astra shell [Tech. Rep. IPP 5/98, Max Plank Institut für Plasmaphysik, Garching, February 2002] was extended by the addition of several peripheral codes that increase the capabilities of transport calculations for plasmas of the TJ-II device (Laboratorio Nacional de Fusión, CIEMAT). Here we document the inclusion of equilibrium calculations and the evolution of the rotational transform, developed later on, informing as well about the calculation methods and providing a short guide for the user.

ACKNOWLEDGEMENTS

We are grateful to A. López-Fraguas and J. Geiger for providing VMEC version 8.46, which admits radial profiles as input.

TABLE OF CONTENTS

LIST OF FIGURES

LIST OF TABLES

1 INTRODUCTION

Transport calculations for the TJ-II stellarator [1] are normally done using the Astra suite [2]. The flexibility of Astra to include user-made subroutines has been exploited to couple specialized codes for the evaluation of source terms, neoclassical electric fields etc. [3]. As mentioned in this last report, one remaining task was the inclusion of equilibrium calculations so that metric-related magnitudes could be adapted to the plasma evolution. The present work is devoted to describe how this has been done and to show some illustrative calculations. It is based on the concept of "susceptance matrix" [4] recalled in Section 2. In Section 3 we explain how the evolution of the rotational transform is done for TJ-II calculations using the Astra frame, which is based on modifications to two main procedures: VMEC and its extension BOOZ_XFORM to obtain Boozer coordinates (3.1), used for updating the elements of the susceptance matrix; and (3.2) an Astra plug-in subroutine developed to make the actual evolution of the rotational transform within Astra. Section 4 provides some examples of calculations using these methods and, finally, Section 5 is a short user-guide with practical purposes. Appendix A is a brief reminder of theoretical aspects that can be found in the literature, and has been included to ease the understanding of the procedures, particularly the modifications to VMEC and BOOZ_XFORM explained in Appendix B.

2 SUSCEPTANCE MATRIX FOR TJ-II CALCULATIONS

Magnetic coordinates are appropriate for theoretical work because they naturally relate the metric properties with physical magnitudes. This is the case for the evolution of the rotational transform, or the plasma current density, in a three-dimensional configuration like that of stellarators, which can be written in terms of the so-called "susceptance matrix" whose elements are more easily found in magnetic coordinates. A brief reminder about magnetic coordinates is given in Appendix A.

The integral form of Ampère's law relates the current through a section with the circulation of the magnetic field along a circuit encircling that section. An expression for Ampère's law suitable for magnetic confinement studies can be found in terms of the poloidal, χ, and toroidal, ϕ, fluxes defined in Eq 14 and Eq 15 in Appendix A. The currents are linearly related with the fluxes through the susceptance matrix S [4] with elements S_{ij}, which is built entirely in terms of the metrics,

$$\mu_0 \begin{pmatrix} I \\ F \end{pmatrix} = \begin{pmatrix} S_{11} & S_{12} \\ S_{21} & S_{22} \end{pmatrix} \begin{pmatrix} \chi' \\ \phi' \end{pmatrix}. \qquad \text{Eq 1}$$

Here the primes indicate derivative with respect to the chosen radial coordinate, namely ρ. Here the poloidal current associated to the poloidal angle θ is defined as the integral including the coil currents [4],

$$F(\rho) = \int_0^{2\pi} \mathrm{d}\xi \int_\rho^\infty \mathrm{d}\rho \, \mathcal{J} J_\theta, \qquad \text{Eq 2}$$

where ξ is the toroidal angular coordinate and $\mathcal{J}$ is the Jacobian that corresponds to the (ρ, θ, ξ) coordinate system.

The rotational transform (Eq 19), according to Eq 1, can be obtained inverting the susceptance matrix,

$$\iota = \frac{\chi'}{\phi'} = \frac{S_{22} I - S_{12} F}{S_{11} F - S_{21} I} \qquad \text{Eq 3}$$

from where a simple expression can be obtained for the vacuum value ($I = 0$):

$$\iota_I = 0 = -\frac{S_{12}}{S_{11}} \qquad \text{Eq 4}$$

Note also that Eq 3 gives a boundary condition ι_a in terms of an equilibrium calculation and a known net plasma current I, which is a typical experimental input.

The elements of S adopt the following form if (ρ, θ, ξ) are magnetic coordinates,

$$\begin{pmatrix} S_{11} & S_{12} \\ S_{21} & S_{22} \end{pmatrix} = \frac{V'}{4\pi^2} \begin{pmatrix} \langle \frac{g_{\theta\theta}}{\mathcal{J}^2} \rangle & \langle \frac{g_{\theta\xi}}{\mathcal{J}^2} \rangle \\ \langle \frac{g_{\xi\theta}}{\mathcal{J}^2} \rangle & \langle \frac{g_{\xi\xi}}{\mathcal{J}^2} \rangle \end{pmatrix}, \qquad \text{Eq 5}$$

where the angle-brakets refer to flux-surface averages. In more general coordinates, the S_{ij} include also derivatives of a periodic function λ (Eq 13 and Eq 16) with respect to the angular

coordinates [4]. Under flux-surface averaging the contribution of such derivatives may be small, but obtaining the susceptance elements Eq 5 with non-magnetic coordinates, such as those of the "g3d" library commonly used for TJ-II calculations ([5], [6]), would yield inaccurate values of the rotational transform Eq 4. In order to give an idea of the differences, the calculations of the susceptance matrix Eq 5 from the nonmagnetic coordinates of the "g3d" library and from Boozer (magnetic) coordinates are compared in Figure 1. It is actually found that the differences in the S_{ij} are small. In the report Ref. [6], this proximity was used to obtain first estimates of the evolution of the rotational transform in TJ-II discharges, even though the relation Eq 4 for the vacuum ι results in more than a 15% difference between "g3d" and magnetic coordinates.

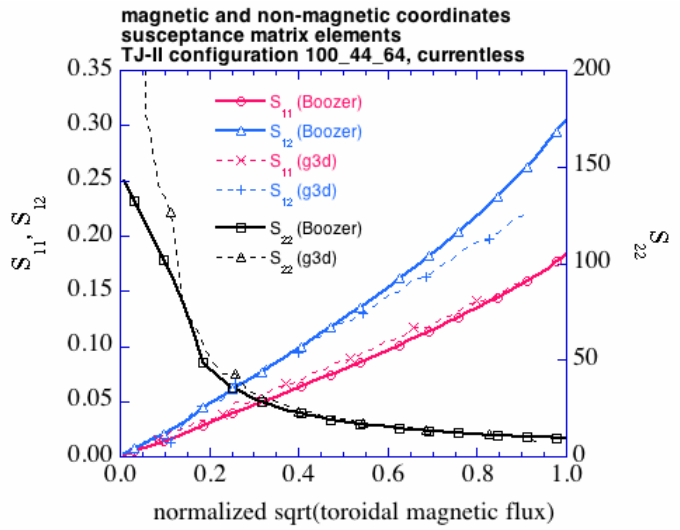

Figure 1. Comparison of the susceptance matrix elements for the vacuum TJ-II configuration 100_44_64 using Eq 5 with magnetic —Boozer— coordinates, and (inappropriate) non-magnetic —g3d— coordinates. The values near the magnetic axis are obtained by linear extrapolation.

Note that, after flux surface averaging, the matrix Eq 5 depends only on the chosen radial coordinate. This gives some freedom in order to ease the calculations.

3 USAGE FROM ASTRA

The evolution of the rotational transform in presence of current density profiles —e.g. bootstrap or ohmically induced currents— is an important piece to evaluate transport in a low magnetic shear device like the TJ-II. Several peripheral codes have been incorporated to the Astra package [2] as a "TJ-II specialized" part of the transport analysis [3]. The aim of the present work is to solve for the evolution of the rotational transform, which may require an update of the metrics in case there is a significant change in the plasma pressure or plasma current densities during the evolution. Therefore, there are two aspects to be covered: the update of the MHD equilibrium (for which either ι or the toroidal current density profiles must be given) and the evolution of the current, which in our case is done through Strand&Houlberg's equation for the evolution of the rotational transform [4] adapted to the radial coordinate

$$\rho = a\sqrt{\frac{\phi}{\phi_0}} \qquad \text{Eq 6}$$

typically used in Astra calculations for TJ-II [6]:

$$\frac{\partial \iota}{\partial t} = \frac{\partial \iota}{\partial \rho}\frac{\partial \rho}{\partial t} + \frac{1}{\rho}\frac{\partial}{\partial \rho}\left\{\frac{\eta_{||}}{\mu_0}\rho(\mathrm{S}_{21}\iota + \mathrm{S}_{22})^2\frac{\partial}{\partial \rho}\left[\frac{\mathrm{S}_{11}\iota+\mathrm{S}_{12}}{\mathrm{S}_{21}\iota+\mathrm{S}_{22}}\right] - \frac{\eta_{||}a^4}{4\phi_0^4\rho}\mathrm{V}'\langle \mathbf{J}_{\mathrm{f}}\cdot\mathbf{B}\rangle\right\}. \qquad \text{Eq 7}$$

In Eq 6 and Eq 7, a is the minor radius, ϕ_0 is the toroidal magnetic flux at the last closed magnetic surface, $\eta_{||}$ is the parallel plasma resistivity, $\mathbf{J}_{\mathrm{f}}$ is the non-inductive current density and the elements of S are calculated using magnetic coordinates (Eq 5) and the radial coordinate ρ defined in Eq 6.

The usage of the codes that complement Astra with the update of metric coefficients and Eq 7 will be described below. In particular, the one that evolves the rotational transform does not include for now the first term in the rhs of Eq 7. This term is expected to be generally small [4] and negligible in the low β plasmas of the TJ-II stellarator, where there is practically no deformation of the flux surfaces due to plasma effects, $\partial_t \rho \approx 0$.

Now, the task of solving Eq 7 is done via the use of two separate plug-in subroutines in Astra: the one that calls VMEC and updates the geometry (§3.1); and the one that provides the evolution equation for ι (§3.2). One advantage of doing it this way is that the calls to VMEC can be controlled separately: In some cases one only call might be enough, while in others, after appropriate convergence runs, repeated calls with a given frequency will be necessary; or maybe the user is only interested in the VMEC equilibria so the evolution of ι is not necessary.

3.1 UPDATE OF THE SUSCEPTANCE

All configuration-dependent coefficients are updated by calling sequentially VMEC and then a modification of the code BOOZ_XFORM to obtain Boozer coordinates and the related new metric and S_{ij} elements (Eq 5). To run the code from Astra one must include a call to the corresponding subroutine equilVMEC. For example (the line commented with "!" is, of course, not necessary),

```
!  EQUIL_VMEC(S11,S12,S22,V'):delta_t:start:end:interactive_key
EQUIL_VMEC(CAR30,CAR31,CAR32,CAR28):0.05:0.0001::B
```

would make a first calculation at $t = 0.1$ ms and make an update automatically every 50 ms. In this example the S-matrix elements are stored in the Astra arrays CAR30, CAR31 and CAR32, and $V' = \mathrm{d}V/\mathrm{d}\rho$ is stored in CAR28. The following aspects should be kept in mind:

- The user-defined transport model must provide the net toroidal plasma current, I_{pl} (Astra variable IPL), the rotational transform, ι (Astra array MV), and the total plasma pressure. These data will be passed to VMEC when the subroutine equilVMEC is called.

- The requirements for the calculation of Boozer coordinates must be written in the input file $HOME/drvmec/input_astra.boz as will be seen below. This file contains information about the flux surfaces from the VMEC output that the conversion code will use to find the new coordinates etc. The file: $HOME/drvmec/input_astra.boz also contains the name of the VMEC output that the conversion code will read, named wout_astra.txt.

- The Astra subroutine equilVMEC calls VMEC. In summary, equilVMEC acts as follows

  - Executes the system directives

    ```
    cd $HOME/drvmec
    cp input.config.100_44_64 input.astra
    ```

    This is because (see below) VMEC will take input.astra as input file. Therefore the user must decide upon what input file is to be used. In this example we have chosen the input file input.config.100_44_64.

  - Substitutes the new pressure and rotational transform profiles (as passed by Astra), and the value of the net current, in the input file input.astra. This allows updating such magnitudes during the transport calculations.

  - Executes VMEC and BOOZ_XFORM, the code to convert to Boozer coordinates. This is done by a system call that executes the script

    $HOME/drvmec/tarea,

    which contains the commands

    ```
    ../bin/xvmec2000 input.astra
    ../bin/xbooz_xform input_astra.boz
    ```

- The output from the code xbooz_xform is writen in the text file: $HOME/drvmec/metrics_average so its values can be used in the next steps of the Astra calculations.

The information contained in the file metrics_average consists of radial profiles for all the magnitudes summarized in Table 1. Observe that the metric coefficients are given in the VMEC radial coordinate s, while the S_{ij} elements and V' are calculated using $\rho = a\sqrt{s}$ (Eq 6) in accordance with the evolution equation 7. The relation $S_{ij}(\rho) = (d\rho/ds)S_{ij}(s)$ holds.

COLUMN	VARIABLE	MEANING
1	jrad	Index of the magnetic flux surface
2	s	Radial coordinate, $s=\phi/\phi_{max}$
3	$S_{11}(\rho)$	Susceptance matrix element, see Eq 5
4	$S_{12}(\rho)$	Id.
5	$S_{22}(\rho)$	Id.
6	g_{ss}	Metric tensor component $\partial_s x \cdot \partial_s x$
7	$g_{s\theta}$	Id. $\partial_s x \cdot \partial_\theta x$
8	$g_{s\xi}$	Id. $\partial_s x \cdot \partial_\xi x$
9	$g_{\theta\theta}$	Id. $\partial_\theta x \cdot \partial_\theta x$
10	$g_{\theta\xi}$	Id. $\partial_\theta x \cdot \partial_\xi x$
11	$g_{\xi\xi}$	Id. $\partial_\xi x \cdot \partial_\xi x$
12	ι	Rotational transform (VMEC output)
13	I	Toroidal current [A (x $\mu_0/2\pi$)], Eq. 26
14	F	Polidal current [A (x $\mu_0/2\pi$)], Eq. 2
15	V'	dV/dρ [m^2]
16	dV	Incremental volume [m^3]

Table 1. Output of the code xbooz_xform in the text file metrics_average. The coordinates are: θ (poloidal Boozer angle); ξ (toroidal Boozer angle); ϕ (toroidal magnetic flux); $\rho = a\sqrt{s}$ where a [m] is the average minor radius of the magnetic configuration.

The VMEC output[1] gives the currents I and F (Eq 2) in Amperes except for a factor $\mu_0/2\pi$. Therefore, to take these currents into Astra they must be converted to MA. For example, the toroidal plasma current should be I_{pl} [MA] = $10^{-6}2\pi I/\mu_0 = 5I$.

In the present version of the subroutine equilVMEC, the metric coefficients and V' are read but not updated into the Astra system. The reason is that such coefficients, even for the highest plasma-β cases reached in TJ-II plasmas, are practically unchanged with respect to the vacuum values. In consequence, their update is not meaningful in practice. Additionally, the radial coordinate in Astra (the one used by diagnosticians and many codes that work with radial profiles) is taken from the g3d library previously mentioned, which may give a radial coordinate ρ_{g3d} and metric coefficients slightly different from the corresponding coordinate from VMEC, that is, $\rho_{\mathrm{g3d}} \approx \sqrt{s}$. This means that a first call to VMEC and the corresponding update of metric coefficients would give a fake change

[1] Under VMEC version 8.46

in the evolution of transport magnitudes, simply due to the small change in radial coordinate. Still, it might become eventually useful doing this update from the beginning so the metrics from g3d are substituted by metrics from VMEC during all calculations. For this reason, the subroutine equilVMEC is ready for this change. All that is needed is redefining the metric coefficients that involve derivatives with respect to s (see Table 1). Recalling that $\mathrm{d}s/\mathrm{d}\rho = 2\rho/a^2$, we simply have

$$g_{\rho\rho} = \frac{4\rho^2}{a^4} g_{ss} \qquad \text{Eq 8}$$

$$g_{\rho\theta} = \frac{4\rho}{a^2} g_{s\theta} \qquad \text{Eq 9}$$

$$g_{\rho\xi} = \frac{4\rho}{a^2} g_{s\xi} \qquad \text{Eq 10}$$

where $\rho \equiv$ RHO and $a \equiv$ ABC are ready from common blocks in the Astra environment.

3.2 EVOLUTION OF THE ROTATIONAL TRANSFORM

Once V' and the susceptance matrix are obtained, the evolution of $\iota(\rho)$ based on Eq 7 is done with the subroutine IOTAEVOL. An example of inclusion in Astra models is

```
! IOTAEVOL(S11,S12,S22,rhs)
IOTAEVOL(CAR30,CAR31,CAR32,CAR24):
```

where we take as inputs the outputs of our previous call to equilVMEC (see §3.1). The Astra array CAR24 has been chosen to store the rhs of Eq 7. It is required that IOTAEVOL is called at *every* Astra time step.

Due to the structure of Eq 7, the Astra solver cannot be used for the evaluation of the diffusive part in the usual way, i.e., defining transport coefficients for the corresponding magnitude [2], which would be ι in our case. Therefore, the evolution of ι is done using the *rhs* of Eq 7 as a whole source term for a chosen free time-evolving array in Astra. It is important to note that we have fixed this array to be F6 inside IOTAEVOL, so it is mandatory using the same array in the Astra model —this condition might be relaxed in the future. Astra passes internally all functions to IOTAEVOL, except for the elements of S, including the non-inductive sources of current density. An example of recommended usage in the transport model is

```
F6: ; F6=MVX;
F6B=F6B        ! The boundary condition is inside IOTAEVOL
DF6=0.         ! Diffusivity must be null
SF6=CAR24      ! Array CAR24 as rhs of Strand&Houlberg's eqn
MV=F6          ! Update of the iota profile
MU=1.5         ! MU does not evolve. Any positive value is valid
CC=CCSP*(1.-sqrt(2./3.*0.34*RHO/AB));  ! Plasma conductivity
CD=0.0         ! No current drive in this case
```

As noted in the comments (written after the ! sign), here we see that:

- The initial rotational transform is taken from the experimental file (typically the vacuum ι).
- The boundary condition, i.e., the rotational transform at the plasma edge, is defined inside the subroutine IOTAEVOL according to Eq 3.
- The diffusivity in the field F6 is forced to zero.
- The *rhs* of Eq 7 is set as a source for the F6 evolution equation in Astra.
- The Astra array for ι is updated with the evolving F6. This is important also because, in an eventual call to equilVMEC, the updated ι will be used as new input to the MHD equilibrium.
- A formula for the plasma electrical conductivity must be provided.
- Any non-inductive currents must be provided.

The last point in the list above deserves a separate discussion. As Eq 7 indicates, a driven or bootstrap current density (respectively CD and CUBS in notation of the Astra programming language) enters through the flux surface average of the scalar quantity $\mathbf{J}_f \cdot \mathbf{B}$. Since these current densities are expected to come from dedicated calculations, it would be desirable to provide them as such averages. In the present version of the IOTAEVOL subroutine, it is understood that the user provides $\langle \mathbf{J}_\mathrm{f} \cdot \mathbf{B} \rangle$ as CD+CUBS. Additionally, the total magnetic flux ϕ_0 must be provided. A default value is set in the subroutine IOTAEVOL, but it must be edited if a different one is needed. The toroidal magnetic flux at the last closed flux surface for TJ-II configurations is normally calculated with separate codes that take, in turn, the output of magnetic field-line integrators. The values of ϕ_0 are, indeed, an input for VMEC calculations (called PHIEDGE in VMEC version 8.46). At present, the user must be careful to set the same ϕ_0 in equilVMEC.f (where the input file for VMEC is defined) and in iotaevol.f.

4 EXAMPLES

In this section we show some examples of calculations performed with the combination of codes described above. In all cases, the interactive Astra suite is used to control the numerical flow through some appropriate Astra model. They are intended to illustrate the kind of output produced by the codes, show useful comparisons and provide some numerical values that can be of general interest for TJ-II studies.

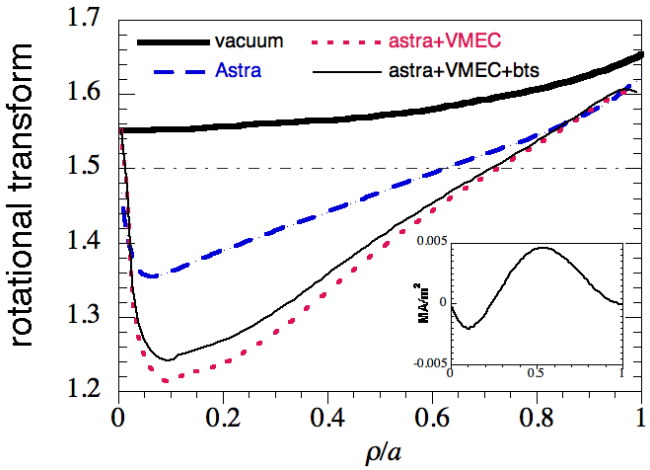

Figure 2. Vacuum ι-profile (black thick line) and comparison of ι-profiles in two calculations with net plasma current I_{pl} = −8 kA: without (red dotted line) and with (thin black line) a bootstrap-current contribution I_{bts} ≈ 0.25 kA with the profile shown in the inset. The grey horizontal line marks the low order rational ι = 3/2. Data from TJ-II discharge #26137 at Thomson Scattering time (skin time ≈ 50 ms).

Figure 2 compares the vacuum rotational transform (black thick line) with the steady state profiles that correspond to a net plasma current I_{pl} = −8 kA, obtained using metric coefficients from VMEC in Eq 7 for two cases: without (thin black line) and with (dotted red line) the addition of a small bootstrap current I_{bts} ≈ 0.25 kA (see its profile in the inset). The bootstrap current term has been obtained in terms of the normalized radial coordinate $\bar{\rho} = \rho/a$ with a formula, $\langle \mathbf{J}_f \cdot \mathbf{B} \rangle = C[3.2(1-\bar{\rho})^2 - 5.5(1-\bar{\rho})^4]\bar{\rho}$, which mimics typical bootstrap current density profiles obtained in electron cyclotron heated plasmas of the TJ-II [[7],[8],[9]]. Using $C = 0.02$ a bootstrap current near 0.25 kA is obtained. As expected, the effect of bootstrap currents is significant only near the magnetic axis in typical low-density plasmas of the TJ-II heated by microwaves alone.

Figure 3 has been obtained calling VMEC with a negligible I_{pl} = −0.02 kA and using again typical profiles of low density TJ-II plasmas heated by electron cyclotron resonance. In this particular case the toroidal $\beta(0) = 0.19\%$. In the representation of $\iota(\bar{\rho})$ we over-plot the VMEC output and the values obtained from Eq. 3 (see Sec. 5), which, aside from suggesting that S is well calculated, indicates with green crosses the flux surfaces chosen in input_astra.boz to perform the calculations. VMEC inputs using 131 or 301 flux surfaces yield the same profiles.

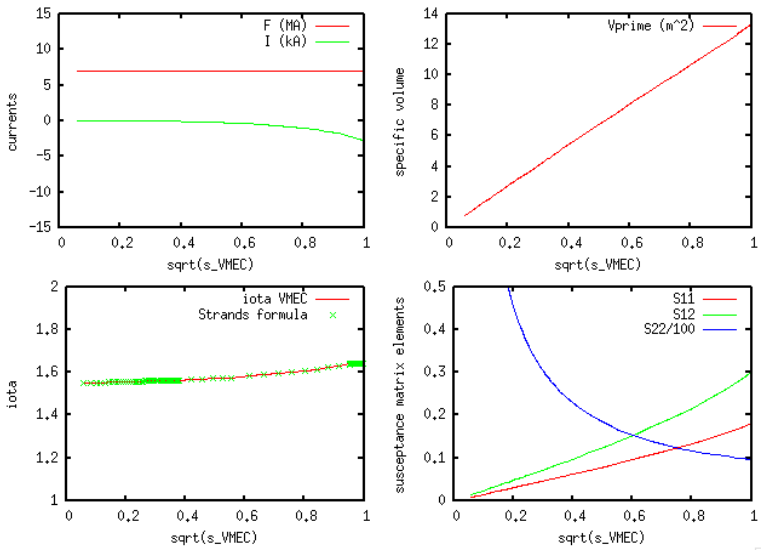

Figure 3. Profiles of plasma current (toroidal, I; poloidal, F), $dV/d\rho$, ι and susceptance matrix elements $S_{ij}(\rho)$ passed to Astra after conversion of VMEC to Boozer coordinates, all of them as a function of $\bar{\rho} = \sqrt{s}$. Values: $\iota_{(a)} = 1.66$, net poloidal current $F(a) = 7016.5$ kA.

Figure 4 shows part of an Astra output panel where we can appreciate the footprint (light blue lines) of the evolution of several profiles during a plasma with ohmic induction up to I_{pl} = −12 kA. In particular, note that slightly different ion density, n_i (left top), and electron temperature (right top), profiles have contributed to the evolution. We have highlighted the final profiles in red. Also shown is the evolution of ι from the vacuum profile when $I_{pl} \approx 0$ to the final profile after the induction process, when the current is maximum and opposing the magnetic field direction.

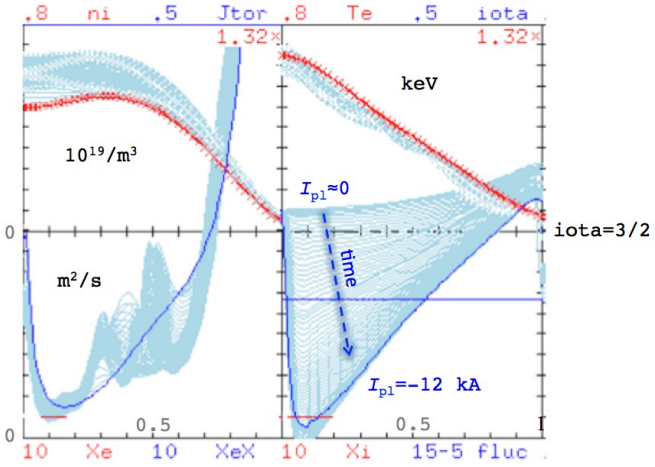

Figure 4. Evolution in time (light blue lines) of ion density, electron temperature, electron diffusivity χ_e and rotational transform starting from zero current until I_{pl} = −12 kA (n_i and T_e, red lines with crosses; χ_e and ι, blue lines). The scales of the ordinates are given at the top and bottom. Calculation based on data from TJ-II discharge #29778.

The evolution of the rotational transform in ohmic induction experiments can be used to estimate the radial location of magnetic resonances (low order rational values of ι), where magnetic islands or other magneto-hydrodynamic phenomena are prone to occur. Figure 5, based on the calculation

shown in Figure 4, is an example of this kind of result: several magnetic resonances enter or exit the plasma, or simply displace through minor radius during the evolution. This calculation serves also to show that VMEC calculations may eventually end without converging. In these cases the calculation is interrupted until the next call to VMEC, when the evolution proceeds. It has been found that these failed runs practically do not affect the general time evolution of ι unless they are very frequent, in which case it might be necessary to modify the VMEC input. For the case of Figure 5, we have used a VMEC input with common TJ-II settings for accuracy, number of modes etc. In particular, the first lines of such input are

```
&INDATA
MGRID_FILE = 'NONE'
LOPTIM = F LOLDOUT = T
DELT = 0.9937378889958275
TCON0 = 2.
NFP = 4
NCURR = 0
MPOL = 16                NTOR = 24
NS_ARRAY =21    41    141
NITER =12000
NSTEP = 100
NVACSKIP=8
GAMMA =0.0E+00
FTOL_ARRAY =5.00E-08    5.00-12    1.00E-12
PHIEDGE = 9.60E-02
```

Note that it is a fixed-boundary run (no MGRID file given) and the periodicity of the TJ-II device is exploited. NCURR = 0 forces VMEC to take the ι profile as input instead of the current density profile.

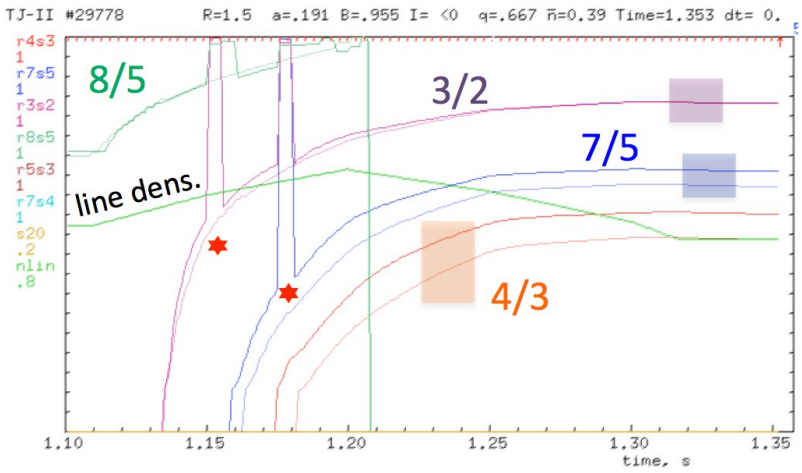

Figure 5. Time evolution of the radial position ($0 \le \bar{\rho} \le 1$) of several rationals labeled with corresponding colours, and the line-density (labeled). VMEC is called every 5 ms of simulated time. Thinner lines (put in correspondence by the rectangles) are the same calculation based on only the initial VMEC call. Red stars

indicate two times at which VMEC does not converge (the vertical lines are an artifact of the plotting in the Astra interface).

Calculations like those of Figure 4 and Figure 5 have been already compared satisfactorily with experimental measurements that give indications of the location of rotating magnetic islands associated to low-order rational values of ι [10]. They represent an improvement of the methods used in [11], which served to relate transport variations with the displacement of low-order rational values of ι throughout the plasma in TJ-II discharges with ohmic induction. For this reason, we present now a comparison of results between the old method and the more accurate procedures here exposed. The top panel in Figure 6 is the time evolution of the electron temperature profile normalized to its mean during the time window, $T_e/\langle T_e \rangle$, a magnitude very sensitive to the movement of rationals (very possibly magnetic islands) in minor radius [12]. The bottom panel is the same except that the calculation of the rational positions in time is done with the methods described in this report, i.e., following a process that we summarize here:

- The ι-profile is taken from the Astra "experimental file" (generally the vacuum one) during the first 0.1 ms of simulated time. Then it evolves according to Eq. 3 using S after the first call to $\mathrm{equilVMEC}$.

- After every call to $\mathrm{equilVMEC}$, the boundary value ι_a is updated according to Eq 3, where F is taken from the file $\$\mathrm{HOME}/\mathrm{drvmec}/\mathrm{metrics\_average}$ (see §3.1). The S_{ij} coefficients are also updated.

- The rhs of Eq 7 (presently, the first term is set to zero) is calculated and the time stepping is done by the Astra kernel.

Former results (e.g. [11], [14], [12]) stressed the experimental fact that low-order rational values of the rotational transform have an effect on plasma profiles, apparently promoting larger temperature gradients or increased temperatures with respect to the average; but it could not be stated wether this happened *at* or *by* the resonant locations. As it can be appreciated from the comparison of the two panels in Figure 6, the qualitative results with the new tools do not change those of the old calculations. In order to address more quantitatively the experimental facts, and aside from more accurate detection methods, refined evaluations of the rotational transform should be done with the present tools. Part of the motivation of this work is the need for such refinements [10].

5 SUMMARY OF USAGE

This last Section compiles the procedure and cautions necessary to run Astra with calls to the equilibrium and ι-evolution subroutines. It is intended to serve as a brief guide to the user. We assume that there exists a file with experimental data for a discharge, where density and temperature profiles are stored at the relevant times (or their boundary conditions in case a transport model makes them evolve). For simplicity, let us suppose that only the evolution of the rotational transform is required giving the experimental net plasma current $I_{\mathrm{pl}}(t)$ as input. The evolution will be calculated using the Astra frame. Therefore, a suited Astra model will be used and here we shall describe only the steps that must be followed to ensure a proper calculation of $\iota(\rho, t)$.

In what follows, the codes VMEC and BOOZ_XFORM are supposed to be in a working directory drvmec. An experimental file TJ2_shotNo is assumed to exist in the Astra working directory.

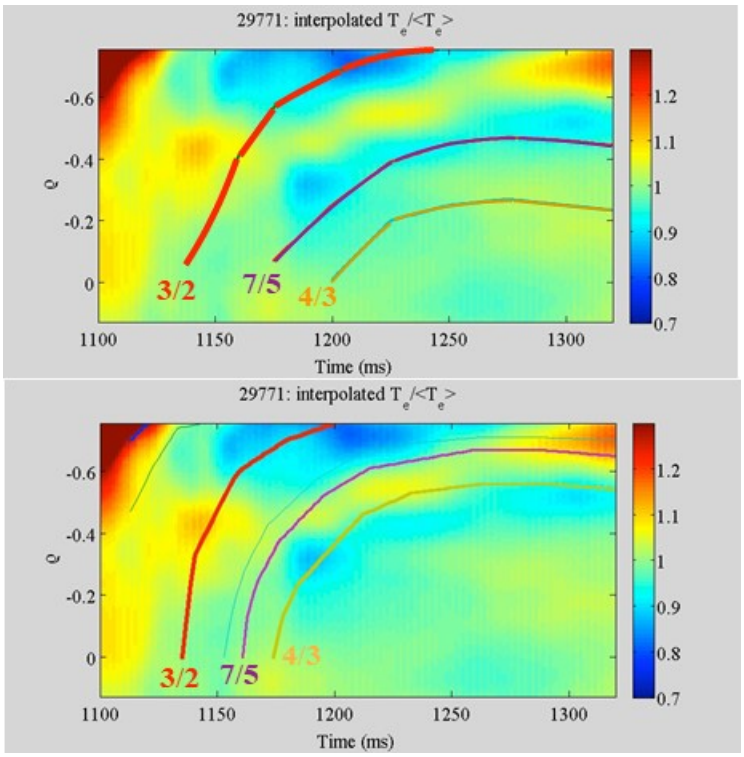

Figure 6. Evolution of the relative variations of the electron temperature (obtained from 11 electron cyclotron emission channels) interpolated in normalized minor radius at the high-field side of the torus, hence the negative values, as the ι-profile evolves due to induced ohmic currents in TJ-II discharge #29771. The lines are the paths followed in time by the indicated low order rationals according to the approximate calculations of [[6], [13], [11]] (top) and the refined calculations using Eq 7 (bottom).

Experimental file requirements. The file TJ2_shotNo must contain, aside from other possible information:

- The time evolution of the net plasma current $I_{\mathrm{pl}}(t)$, provided as several values of the Astra variable IPL at the corresponding times. Astra will interpolate linearly in time the values. The

user must decide how many values are necessary in order to describe properly the experimental evolution of the plasma current.

- The initial $\iota(\rho)$. This will be the first value sent to VMEC for a first calculation of S and is stored as the Astra array MV.

- The metric coefficients G11, G22 and G33 (see Astra manual). At present these remain unchanged (see §3.1); but even if equilVMEC is updated so as to make them evolve, initial values are necessary. Note that the profiles G11, G22 and G33 may be also given at different times in TJ2_shotNo. Astra will use the corresponding linear interpolation in time of these profiles for the transport calculations.

Astra model requirements.

- In the "Grids" window of Astra control variables, the time step might need being limited to guarantee a stable evolution of the evolving array associated to $\iota(\rho, t)$. Recommendable values are TAUMAX = 1e-6; TAUMIN=1e-7, and can be fixed in the Astra model as well.

- The model must force NEQUIL=-1 so the metrics are read from the "experimental file" TJ2_shotNo.

- Calls to the relevant subroutines must exist:

  - *Update of susceptance elements*: Decide arrays to store the updated S, which will be passed to IOTAEVOL also in the model. The user must ensure that the plug-in subroutine EQUIL_VMEC is started at an appropriate time and called frequently enough. In TJ-II calculations, a time interval of about 5 to 10 ms is generally enough.

  - *Evolution of ι:* It is recommended calling the plug-in subroutine IOTAEVOL at every Astra time step.

- Activate evolution equation for auxiliary evolving array F6. In the present version, the use of F6 is mandatory because it is used inside iotaevol.f, which is the source code for IOTAEVOL.

  - Set evolving F6 with initial profile and boundary taken from experimental file, for instance writing F6: ; F6=MVX; F6B=F6B

  - Force zero diffusivity for F6 field, DF6=0.

  - Force right hand side of evolution equation to be the output from IOTAEVOL, for instance SF6=CAR24 if the auxiliary array CAR24 has been used as output of IOTAEVOL.

  - Provide a value for the Astra variable MU (≡ ι) that is positive. This avoids problems when running Astra. For instance, MU=sqrt(MV*MV+1.e-6).

- Provide a formula for the plasma conductivity (Astra array CC).

- Provide non-inductive currents (Astra arrays CD for current drive and CUBS for bootstrap), see §3.2. Astra sets them to zero by default.

Subroutines requirements. In a previous version, the subroutine equilVMEC made use of polinomial expansions of the pressure and ι profiles. This was found to be problematic for the evolving ι. A new version was developed to make use of the new capability of VMEC to handle profiles given by their arguments and values, to which we refer the following points. The option PIOTA_TYPE = 'Akima Spline' has been found most appropriate for ι.

- equilVMEC: Edit the source file equilVMEC.f and search for the commented line "CHANGE MAGNETIC CONFIGURATION HERE" in order to select the right VMEC input for the sought magnetic configuration. It must exist in drvmec.

- IOTAEVOL: The value ϕ_0 of the toroidal flux at the last closed magnetic surface, Psi0m2 in the file iotaevol.f, must be consistent with the value PHIEDGE passed to VMEC via its input file. The reading of the toroidal flux might be made automatic in future versions.

Requirements for VMEC and BOOZ_XFORM

- The call to both codes, VMEC and BOOZ_XFORM, is done using a simple shell script named drvmec/tarea. The user must be sure that the codes are indeed called, since occasionally this script can be used to avoid calling one or both codes for other purposes. As seen in drvmec/tarea, there are arguments to the codes that might require editing:

  - drvmec/input.astra. This is the file where equilVMEC will copy the VMEC input file in run-time. All edits about the number of modes, tolerances etc. must be edited in the VMEC input file (see last item below).

  - drvmec/input_astra.boz. This is the input to BOOZ_XFORM. In a first line, two integers are respectively the number of toroidal and poloidal modes to be used in the calculations, mboz and nboz. These will be redefined depending on the corresponding MPOL and NTOR used in the input to VMEC as follows: mboz = MAX (6*MPOL, 2, mboz), and nboz = MAX (2*NTOR-1, 0, nboz). The second line of the input has the indexes of the flux surfaces for which the results will be given. It is convenient accumulating points near the origin and calculation edge (see Figure 3).

- VMEC input files have names input.p.config.LABEL, where LABEL is the name provided by the user to identify the magnetic configuration. It is recommended checking this input file for details of the calculations (tolerances, number of modes, maximum toroidal flux, type of bounday –fixed/free– etc.) The pressure and ι profiles, and the net plasma current, will be overwritten by equilVMEC during run-time.

6 REFERENCES

[1] Alejaldre C, Alonso J J, Botija J, Castejon F, Cepero J R, Guasp J, Lopez-Fraguas A, Garcia L, Krivenski V I, Martin R, Navarro A P, Perea A, Rodriguez-Yunta A, Sorolla M and Varias A 1990 Fusion Technology 17 131–139 URL: http://www.ans.org/pubs/journals/fst/a29176

[2] Pereverzev G V and Yushmanov P N 2002 ASTRA Automated System for TRans- port Analysis Tech. Rep. IPP 5/98 Max Plank Institut für Plasmaphysik, Garching

[3] López-Bruna D, Reynolds J M, Cappa A, Martinell J, García J and Gutiérrez-Tapia C 2010 Programas periféricos de ASTRA para el TJ-II Informes Técnicos Ciemat 1201 CIEMAT URL: http://documenta.ciemat.es/bitstream/123456789/114/1/40921IC1201.pdf

[4] Strand P I and Houlberg W A 2001 Physics of Plasmas 8 2782–2792. URL: https://doi.org/10.1063/1.1366618

[5] Guasp J and Liniers M 2000 Búsqueda de efectos quasi-isodinámicos en el TJ-II Informes Técnicos Ciemat 946 CIEMAT URL http://www-fusion.ciemat.es/InternalReport/IR946.pdf

[6] López-Bruna D, Romero J A and Castejón F 2006 Geometría del TJ-II en ASTRA. 6.0 Informes Técnicos Ciemat 1086 CIEMAT Madrid

[7] Reynolds Barredo J M 2009 Simulación de plasmas mediante las ecuaciones cinéticas de deriva en geometrías complejas Ph.D. thesis Facultad de Ciencias, Universidad de Zaragoza Zaragoza URL http://zaguan.unizar.es/record/4555/?ln=en

[8] Velasco J L, Allmaier K, López-Fraguas A, Beidler C D, Maassberg H, Kernbichler W, Castejón F and Jiménez J A 2011 Plasma Physics and Controlled Fusion 53 115014 URL https://iopscience.iop.org/article/10.1088/0741-3335/53/11/115014

[9] Tribaldos V, Beidler C D, Turkin Y and Maassberg H 2011 Physics of Plasmas 18. 102507 (pages 10) URL: https://doi.org/10.1063/1.3649928

[10] Ochando M A, López-Bruna D and Pedrosa M A 2013 Tracking magnetic resonances through their effect on global radiation signals Joint 19th ISHW and 16th RFP workshop (Padova – Italy) URL:http://www.igi.cnr.it/ishrfpws2013/sites/default/files/attachments/12 BookOfAbstracts.pdf

[11] López-Bruna D, Estrada T, Medina F, de la Luna E, Romero J A, Ascasíbar E, Castejón F and Vargas V I 2008 EPL (Europhysics Letters) 82 65002 URL http://stacks.iop.org/0295-5075/82/i=6/a=65002

[12] López -Bruna D, Pedrosa M A, Ochando M A, Estrada T, van Milligen B P, López- Fraguas A, Romero J A, Baião D, Medina F, Hidalgo C et al. 2011 Plasma Physics and Controlled Fusion 53 124022 URL http://iopscience.iop.org/article/10.1088/0741-3335/53/12/124022/meta

[13] López-Bruna D, Castejón F, Romero J A, Estrada T, Medina F, Ochando M, López- Fraguas A, Ascasibar E, Herranz J, Sánchez E, de la Luna E and Pastor I 2006 Magnetic shear and transport in ECRH discharges of the TJ-II under ohmic induction Tech. Rep. 1089 CIEMAT Madrid URL http://www-fusion.ciemat.es/InternalReport/IR1089.pdf

[14] López-Bruna D, Romero J A, López-Fraguas A, Reynolds J M, Blanco E, Estrada T, Ochando M A, Jiménez-Gómez R, Bondarenko O, Tafalla D, Herranz J, Ascassíbar E, Vargas V I and TJ-II Team 2010 Contributions to Plasma Physics 50 pp 600–604 ISSN 1521-3986. URL: https://doi.org/10.1002/ctpp.

[15] d'Haeseleer W D, Hitchon W N G, Callen J D and Shohet J L 1991 Flux Coordinates and Magnetic Field Structure Scientific Computation (Springer-Verlag)

[16] Hamada S 1962 Nuclear Fusion 2 23–37 URL https://doi.org/10.088%2F0029-5515%2F2%2F1-2%2F005

[17] Boozer A H 1982 The Physics of Fluids 25 520–521 (Preprint URL https://aip.scitation.org/doi/pdf/10.1063/1.863765).

[18] Hirschman S P and C W J 1983 Phys. Fluids 26 3553 URL https://doi.org/10.1063/1.864116

[19] Hirshman S P, van Rij W I and Merkel P 1986 Comput. Phys. Comm. 43 143. URL https://www.sciencedirect.com/science/article/pii/0010465586900585

APPENDIX

A. MAGNETIC COORDINATES: A REMINDER

To ease the reading of this report and establish the notation, we include here a brief reminder about magnetic coordinates (see [15] for a complete reference). Let us assume a triad of appropriate coordinates for a nesting of general toroids, s, θ, ξ, where s is a label for each nested toroid, and θ and ξ are respectively poloidal and toroidal angular —periodic— coordinates. It is desirable that these coordinates are somehow attached to the magnetic geometry. In the case of the "radial" coordinate s one can immediately think of the successive nested toroids associated to magnetic flux tubes and any suitable label for them, like the volume enclosed or the toroidal magnetic flux through their sections. The choice of angular coordinates is less obvious.

The magnetic field $\mathbf{B}$ is, by definition, tangent everywhere to the magnetic flux surfaces, i.e. $\mathbf{B} \cdot \nabla s = 0$. Thus, in general we can write

$$\mathbf{B} = (\mathbf{B} \cdot \nabla\theta)\partial_\theta \mathbf{r} + (\mathbf{B} \cdot \nabla\xi)\partial_\xi \mathbf{r} = B^\theta \partial_\theta \mathbf{r} + B^\xi \partial_\xi \mathbf{r} \qquad \text{Eq 11}$$

where $\mathbf{r}$ is the position vector. A natural procedure to find appropriate angular coordinates is to exploit the constraints on $\mathbf{B}$ itself and the toroidal geometry: $\nabla \cdot \mathbf{B} = 0$ and $\mathbf{B}$ must have periodic components. First, note that the $B^s = 0$ vector

$$\mathbf{B} = \nabla s \times \nabla \alpha \qquad \text{Eq 12}$$

guarantees $\nabla \cdot \mathbf{B} = 0$ for any scalar function $\alpha = \alpha(s, \theta, \xi)$. In general we have $\nabla\alpha = \partial_s \alpha \nabla s + \partial_\theta \alpha \nabla\theta + \partial_\xi \alpha \nabla\xi$, but it is manifest that the ∇s component of $\nabla\alpha$ does not contribute to $\mathbf{B}$ in Eq. 12. With respect to the angular dependencies, the constraint of periodicity allows for the following general functional form for α,

$$\alpha = b(s)\theta + c(s)\xi + \lambda(s, \theta, \xi), \qquad \text{Eq 13}$$

where λ is a periodic function. So to speak, any complicated angular dependency is transferred to λ, but it is in principle possible to find angular coordinates such that $\lambda = 0$ everywhere. In this case the contour map representation of α on the (θ, ξ) plane consists of straight lines coincident with the magnetic field lines themselves. Even if $\lambda \neq 0$ and so the representation does not consist of straight lines, it is easy to realize that α is a label for each appearance of a magnetic field line in the (θ, ξ) plane.

Using the definitions for toroidal and poloidal magnetic fluxes[2], respectively

[2] A toroidal surface is obtained in the corresponding domain at constant ξ and is then perpendicular to $\nabla\xi$ everywhere; the poloidal surface is defined analogously.

$$\phi(s) = \iint_{\text{toroidal suface}} \mathbf{B} \cdot \mathrm{d}\mathbf{S} \qquad \text{Eq 14}$$

$$\chi(s) = \iint_{\text{poloidal suface}} \mathbf{B} \cdot \mathrm{d}\mathbf{S}, \qquad \text{Eq 15}$$

it is not difficult to find [15] that $b(s) = (1/2\pi)\phi'$ and $c(s) = -(1/2\pi)\chi'$ (the prime means derivative with respect to the argument and the 2π factors appear because we are considering that the angles are periodic in the $[0, 2\pi]$ interval), so from Eq. 13 the function

$$\alpha(s, \theta, \xi) = \frac{\phi'(s)}{2\pi}\theta + \frac{\chi'(s)}{2\pi}\xi + \lambda(s, \theta, \xi). \qquad \text{Eq 16}$$

When the angular coordinates are chosen to impose $\lambda = 0$ in Eq 16, the set $\{s, \theta, \xi\}$ is called *magnetic coordinates*. Then the magnetic field Eq. 12 admits the general form

$$\mathbf{B} = \frac{\phi'}{2\pi}\nabla s \times \nabla\theta + \frac{\chi'}{2\pi}\nabla\xi \times \nabla s, \qquad \text{Eq 17}$$

which is referred to as *contravariant* because, as one can see using the geometric relationships $\mathcal{J}\nabla s \times \nabla\theta = \partial_\xi \mathbf{r}$ and $\mathcal{J}\nabla\xi \times \nabla s = \partial_\theta \mathbf{r}$, an expression like Eq 11 is immediately recovered where $B^\theta = \chi'/(2\pi\mathcal{J})$ and $B^\xi = \phi'/(2\pi\mathcal{J})$. Here, $\mathcal{J} = (\nabla s \cdot \nabla\theta \times \nabla\xi)^{-1}$ is the Jacobian of the magnetic coordinates.

Recall that ϕ itself is a valid flux surface label; if taken as a coordinate, the magnetic field becomes

$$\mathbf{B} = \frac{1}{2\pi}\nabla\phi \times \nabla\theta + \frac{\iota}{2\pi}\nabla\xi \times \nabla\phi \qquad \text{Eq 18}$$

where the flux surface quantity

$$\iota(\phi) = \frac{\mathrm{d}\chi}{\mathrm{d}\phi} \qquad \text{Eq 19}$$

is called *rotational transform*[3]. Thus, for a given flux surface, in magnetic coordinates the toroidal flux ϕ is completely determined by the poloidal flux χ.

When $\lambda \neq 0$ in Eq 16 the set $\{s, \theta, \xi\}$ does not correspond to magnetic coordinates and the magnetic field does not admit the pure contravariant expression Eq 17. To find magnetic coordinates from this set one needs only act on the original angular ones, i.e., the role of *s* is not important as long as it is a flux surface label. Moreover, one of the angular coordinates can be fixed and then, upon transforming the other one, a set of magnetic coordinates can be obtained. It is common practice fixing ξ to be coincident with the cylindrical angle and then defining θ so as to obtain $\lambda = 0$.

[3] Since $\chi' = \left(\frac{\mathrm{d}\chi}{\mathrm{d}\phi}\right)\phi' = \iota\phi'$, the definition $\iota = \chi'/\phi'$ is often found in the literature.

Inspecting Eq 16, two options to construct magnetic coordinates $(s, \theta_{\mathrm{m}}, \xi_{\mathrm{m}})$ are found: either fix $\xi_{\mathrm{m}} \equiv \xi$ and change θ to the new

$$\theta_{\mathrm{m}} \equiv \theta + 2\pi\lambda/\phi' \,, \qquad \text{Eq 20}$$

or work analogously preserving $\theta_{\mathrm{m}} \equiv \theta$ and defining

$$\xi_{\mathrm{m}} \equiv \xi - 2\pi\lambda/\chi'. \qquad \text{Eq 21}$$

From now on, let $\{s, \theta, \xi\}$ be a set of magnetic coordinates so that $\alpha = \left(\frac{\phi'}{2\pi}\right)\theta - (\chi'/2\pi)\xi$ and the contravariant expression 17 holds. What change of coordinates preserves the $\lambda = 0$ condition? If $g(s, \theta, \xi)$ is another well-behaved and periodic function, after direct substitution we see that the new coordinates

$$\theta^* = \theta - g(s, \theta, \xi)\chi' \qquad \text{Eq 22}$$

$$\xi^* = \xi - g(s, \theta, \xi)\phi', \qquad \text{Eq 23}$$

are also magnetic. Since ϕ and χ are related by the rotational transform, an alternative way is to define another periodic function $\omega(s, \theta, \xi) = g(s, \theta, \xi)\phi'$ and rewrite the previous expressions

$$\theta^* = \theta - \iota\omega(s, \theta, \xi) \qquad \text{Eq 24}$$

$$\xi^* = \xi - \omega(s, \theta, \xi). \qquad \text{Eq 25}$$

An analogous process can be applied to the current density $\mathbf{J}$ because it is also divergence free and the same considerations as for the magnetic field apply. Instead of the toroidal and poloidal magnetic fluxes (Eq 14 and Eq 15) it is now convenient to define the corresponding surface integrals

$$I = \iint_{\text{toroidal surface}} \mathbf{J} \cdot \mathrm{d}\mathbf{S} \qquad \text{Eq 26}$$

$$G = \iint_{\text{poloidal surface}} \mathbf{J} \cdot \mathrm{d}\mathbf{S} \qquad \text{Eq 27}$$

which have the respective physical meanings of toroidal and poloidal current. Here the integral of G is taken on a ribbon that extends from the magnetic axis to the flux surfaces. Alternatively, it can be defined as the radial integral from the magnetic surface to infinity as in Eq 2, where we have written F instead of G to distinguish. The relationship between both definitions of the poloidal current for fixed magnetic surfaces is $\mathrm{d}G = -\mathrm{d}F$ or, equivalently, $\nabla G = -\nabla F$ [15].

Considering $\mathbf{J} = \nabla\phi \times \nabla\alpha_J$ with a function $\alpha_J = h\theta + i\xi + \lambda_J$ analogous to Eq. 13, we obtain

$$\alpha_J = \frac{I'}{2\pi}\theta - \frac{G'}{2\pi}\xi + \lambda_J(\phi,\theta,\xi) \qquad \text{Eq 28}$$

Despite having assumed that $\{\phi,\theta,\xi\}$ are magnetic coordinates ($\lambda = 0$), nothing guarantees that $\lambda_J = 0$ everywhere. Then, although the coordinates are magnetic, the current density adopts the general form

$$J = \frac{I'}{2\pi}\nabla\phi\times\nabla\theta + \frac{G'}{2\pi}\nabla\xi\times\nabla\phi + \nabla\phi\times\nabla\lambda_J(\phi,\theta,\xi) \qquad \text{Eq 29}$$

or, grouping terms,

$$J = \left(\frac{I'}{2\pi} + \partial_\theta\lambda_J\right)\nabla\phi\times\nabla\theta + \left(\frac{G'}{2\pi} - \partial_\theta\lambda_J\right)\nabla\xi\times\nabla\phi \qquad \text{Eq 30}$$

The relationship among the vector fields, $\mu_0\mathbf{J} = \nabla\times\mathbf{B}$, allows to find explicit relationships between the functions entering the expressions for $\mathbf{B}$ and $\mathbf{J}$. Since the curl relates contravariant components of $\mathbf{J}$ with covariant components of $\mathbf{B}$,

$$\mu_0\,\mathcal{J}J^\phi = 0 = \partial_\theta B_\xi - \partial_\xi B_\theta \qquad \text{Eq 31}$$

$$\mu_0\mathcal{J}J^\phi = \mu_0\left[\frac{G'}{2\pi} - \partial_\xi\lambda_J\right] = \partial_\xi B_\phi - \partial_\phi B_\xi \qquad \text{Eq 32}$$

$$\mu_0\mathcal{J}J^\xi = \mu_0\left[\frac{I'}{2\pi} - \partial_\theta\lambda_J\right] = \partial_\phi B_\theta - \partial_\theta B_\phi, \qquad \text{Eq 33}$$

these equations can be solved for the covariant components[4] to obtain

$$B_\phi = -\mu_0\lambda_J + \partial_\phi\zeta \qquad \text{Eq 34}$$

$$B_\theta = \frac{\mu_0}{2\pi}I + \partial_\theta\zeta \qquad \text{Eq 35}$$

$$B_\xi = -\frac{\mu_0}{2\pi}G + \partial_\xi\zeta \qquad \text{Eq 36}$$

for a new periodic function $\zeta(\phi,\theta,\xi)$. Then the general covariant form of $\mathbf{B}$ is expressed in terms of the toroidal and poloidal currents,

$$\mathbf{B} = \frac{\mu_0}{2\pi}\left(-2\pi\lambda_J\nabla\phi + I\nabla\theta - G\nabla\xi\right) + \nabla\zeta \qquad \text{Eq 37}$$

We observe that the "radial" component in the covariant representation is not necessarily zero. The function λ_J can be obtained from the MHD equilibrium condition $\nabla p = \mathbf{J}\times\mathbf{B}$ if the pressure profile $p(\phi)$ is given. In addition, the covariant representation is not simple because of the function ζ.

[4] The process is not immediate, but not difficult either. It exploits again the bi-periodicity of the torus.

The contravariant form of the magnetic field in magnetic coordinates (Eq 17), or its version using the toroidal flux as flux surface label (Eq 18), is preserved if the angular coordinates are transformed like in Eq 24 and Eq 25. How do these transformations affect the covariant form Eq. 37? After direct substitution of the transformed angles it is found that such form is preserved,

$$\mathbf{B} = \frac{\mu_0}{2\pi}\left(-2\pi\lambda_J^*\nabla\phi + I\nabla\theta^* - G\nabla\xi^*\right) + \nabla\zeta^*\,, \qquad \text{Eq 38}$$

where the functions $\zeta^* = \zeta + (\iota I - G)\omega$ and $\lambda^* = \lambda_J + \omega(\iota I' - G')$ have been defined. Therefore, under suitable angular coordinate changes it is in principle possible to find magnetic coordinates that satisfy different properties. For example, if $\lambda^* = 0$, pure contravariant expressions are obtained simultaneously for the magnetic field and the current density (Eq 29) so the field lines are straight in the $\{\theta, \xi\}$ plane for both $\mathbf{B}$ and $\mathbf{J}$ —such are Hamada coordinates [16]. On the other hand, if the coordinate change makes $\zeta^* = 0$, the magnetic field has simple covariant and contravariant representations, as is the case of the set of Boozer coordinates [17] that have been used in this work.

B. BOOZ_XFORM MODIFICATIONS DETAILS

B1. INTRODUCTION TO VMEC

VMEC is an ideal equilibrium code based on variational methods [[18],[19]] that can work both on fixed or free boundary. The code uses a spectral discretization in the angular coordinates and finite differences for the radial coordinate. It assumes nested magnetic surfaces, based on a Lagrangian grid whose nodes correspond topologically with the magnetic surfaces. Based on a variational approach, the node positions are evolved on a virtual time until a local minimum for the total energy

$$W = \int \left(\frac{|B|^2}{2\mu_0} + \frac{p}{\gamma - 1}\right) \mathrm{d}^3 x \qquad \text{Eq 39}$$

is found. Here, $\gamma > 0$ is the adiabatic index. Both the mass and the magnetic flux are conserved during the process, which is constrained to a particular profiles for the pressure and either ι or the toroidal current density. The minimum of W, where the gradient of the energy is zero, corresponds with the *zero* forces equilibrium:

$$\mathbf{J} \times \mathbf{B} + \nabla p = 0 \qquad \text{Eq 40}$$

$$\nabla \times \mathbf{B} = \mu_0 \mathbf{J} \qquad \text{Eq 41}$$

$$\nabla \cdot \mathbf{B} = 0. \qquad \text{Eq 42}$$

The magnetic field is expressed as

$$\mathbf{B}(s, \theta_v, \zeta_v) = \nabla \phi(s) \times \nabla [\theta_v + \lambda_v(s, \theta_v, \zeta_v)] + \iota(s) \nabla \zeta_v \times \nabla \phi(s), \qquad \text{Eq 43}$$

where we use the nomenclature of the original references: s is the radial coordinate (toroidal magnetic flux normalized to the value at the boundary), θ_v and ζ_v are the (non-magnetic) poloidal and toroidal angular coordinates, respectively. The toroidal VMEC coordinate ζ_v is exactly equivalent to the cylindrical toroidal coordinate. The free periodic function $\lambda_v(s, \theta_v, \zeta_v)$, equivalent to $2\pi\lambda/\phi'$ in Eq 20, is chosen in VMEC so as to optimize the spectral basis for the angular coordinates; i.e., under the VMEC choice, the truncated Fourier series used for the discretization is the most accurate possible. Since $\theta_v + \lambda_v$ is a magnetic coordinate, we can relate the VMEC and Boozer coordinates using Eq 22 and Eq 23 with an appropriate function g_{B},

$$\theta_{\mathrm{B}} = \theta_v + \lambda_v(s, \theta_v, \zeta_v) + g_{\mathrm{B}}(s, \theta_v, \zeta_v) \chi' \qquad \text{Eq 44}$$

$$\zeta_{\mathrm{B}} = \zeta_v + g_{\mathrm{B}}(s, \theta_v, \zeta_v) \phi', \qquad \text{Eq 45}$$

which can be also written ($P \equiv -\omega$ in Eq 24 and Eq 25) as:

$$\theta_{\mathrm{B}} = \theta_v + \lambda_v(s, \theta_v, \zeta_v) + \iota(s) P(s, \theta_v, \zeta_v) \quad \text{Eq 46}$$

$$\zeta_{\mathrm{B}} = \zeta_v + P(s, \theta_v, \zeta_v) \quad \text{Eq 47}$$

where

$$P(s, \theta_v, \zeta_v) = \phi'(s) g_{\mathrm{B}}(s, \theta_v, \zeta_v). \quad \text{Eq 48}$$

The code BOOZ_XFORM effectuates this transformation and offers the VMEC solution in Boozer coordinates, including most of the metrics coefficient details. However, neither the coefficient g_{ss} in Boozer coordinates nor the surface average of the metric coefficients are calculated. Here, we will show the details associated with these small additions to the code, required for the main topic of this work. But first, some insight into the VMEC discretization will be given.

B2. DISCRETIZATION DETAILS

As mentioned above, VMEC uses a spectral expansion in the angular coordinates and a finite difference grid on the radial direction. The topology of the domain corresponds with a set of nested flux surfaces, and the cylindrical coordinates associated with each i-th magnetic surface, under stellarator symmetry[5], is

$$R(s_i, \theta_v, \zeta_v) = \sum_{m=0}^{N_p} R_v^{mO}(s_i) \cos(m\theta_v) + \sum_{n=1}^{N_t} \sum_{m=-N_p}^{N_p} R_v^{mn}(s_i) \cos\left(m\theta_v - nN_{\mathrm{fp}}\zeta_v\right) \quad \text{Eq 49}$$

$$Z(s_i, \theta_v, \zeta_v) = \sum_{m=0}^{N_p} Z_v^{mO}(s_i) \sin(m\theta_v) + \sum_{n=1}^{N_t} \sum_{m=-N_p}^{N_p} Z_v^{mn}(s_i) \sin\left(m\theta_v - nN_{\mathrm{fp}}\zeta_v\right) \quad \text{Eq 50}$$

where N_p and N_t are the number of poloidal and toroidal Fourier modes used on the discretization (a finite truncation is required in order to do numerical calculations), N_{fp} is the number of symmetric field periods. The values of $s_i = (i-1)\Delta s$ for $i \in [1, N_s]$ correspond to the N_s nodes of the radial grid, with spacing $\Delta s = 1/(N_s - 1)$. Of course, s_1 corresponds to the magnetic axis and s_{N_s} to the boundary magnetic surface.

According to VMEC nomenclature this radial grid is referred to as *full grid*. On the other side, quantities like the $\lambda_v(s, \theta_v, \zeta_v)$ are defined on the *half grid* as:

$$\lambda_v\left(s_{i-1/2}, \theta_v, \zeta_v\right) = \sum_{m=0}^{N_p} \lambda_v^{mO}(s_i) \sin(m\theta_v) + \sum_{n=1}^{N_t} \sum_{m=-N_p}^{N_p} \lambda_v^{mn}(s_i) \sin\left(m\theta_v - nN_{\mathrm{fp}}\zeta_v\right) \quad \text{Eq 51}$$

where $s_{i-1/2} = (i - 1/2)\Delta s$ for $i \in [2, N_s]$ and again stellarator symmetry is assumed.

[5] VMEC can also work under the most general case of non-stellarator symmetry, but such extra complexity is not required for TJ-II and will be ignored on the derivations. However, the extension should be trivial.

An extra complication of the discretization is that VMEC splits spatial functions, say $X(s,\theta,\zeta)$, on their even and odd parts,

$$X(s,\theta,\zeta) = X^{\mathrm{e}}(s,\theta,\zeta) + \sqrt{s}\, X^{\mathrm{o}}(s,\theta,\zeta). \quad \text{Eq 52}$$

This splitting helps to have a better behaviour of the functions and their radial derivatives near the magnetic axis, where the transformation is singular. The even part of the expression is associated with the even poloidal Fourier modes and the odd part with the odd poloidal modes divided by $\sqrt{s}$. As an example, the R coordinate can then be split as

$$R(s,\theta,\zeta) = R^{\mathrm{e}}(s,\theta,\zeta) + \sqrt{s}\, R^{\mathrm{o}}(s,\theta,\zeta) \quad \text{Eq 53}$$

with

$$R^{\mathrm{e}}(s_i,\theta_v,\zeta_v) = \sum_{m\ \mathrm{even}}^{[-N_p,N_p]} R_v^{m0}(s_i)\cos(m\theta_v) + \sum_{n=1}^{N_t}\sum_{m\ \mathrm{even}}^{[-N_p,N_p]} R_v^{mn}(s_i)\cos\left(m\theta_v - nN_{\mathrm{fp}}\zeta_v\right) \quad \text{Eq 54}$$

$$R^{\mathrm{o}}(s_i,\theta_v,\zeta_v) = \sum_{m\ \mathrm{even}}^{[-N_p,N_p]} \frac{R_v^{m0}(s_i)}{\sqrt{s_i}}\cos(m\theta_v) + \sum_{n=1}^{N_t}\sum_{m\ \mathrm{odd}}^{[-N_p,N_p]} \frac{R_v^{mn}(s_i)}{\sqrt{s_i}}\cos\left(m\theta_v - nN_{\mathrm{fp}}\zeta_v\right) \quad \text{Eq 55}$$

Sometimes, it is required knowing in the *half* mesh the value of a quantity X defined on the *full* mesh. Then

$$\{X\}_{i-1/2} = \{X^{\mathrm{e}}\}_{i-1/2} + \left\{\sqrt{s}\right\}_{i-1/2}\{X^{\mathrm{o}}\}_{i-1/2} = \langle X^{\mathrm{e}}\rangle_{i-1/2} + \sqrt{s_{i-1/2}}\,\langle X^{\mathrm{o}}\rangle_{i-1/2} \quad \text{Eq 56}$$

where $\{X\}_{i-1/2}$ means evaluation of the function on $s_{i-1/2}$, and

$$\langle \mathrm{X}^{\mathrm{e,o}}\rangle_{i-1/2} = \frac{\{\mathrm{X}^{\mathrm{e,o}}\}_{i+1} - \{\mathrm{X}^{\mathrm{e,o}}\}_{i-1}}{2} \quad \text{Eq 57}$$

This way of working with the quantities keeps the same analytic behaviour of the original quantities near the axis. A similar process is followed for the radial derivative

$$\left.\frac{\partial X}{\partial s}\right|_{s_{i-1/2}} \equiv \{X_s\}_{i-1/2} = \left\{\left(X^{\mathrm{e}} + \sqrt{s}X^{\mathrm{o}}\right)_s\right\}_{i-1/2} = \left\{X^{\mathrm{e}} + \frac{1}{2\sqrt{s}}X^{\mathrm{o}} + \sqrt{s}X_s^{\mathrm{o}}\right\} = \{X_s^{\mathrm{o}}\}_{i-1/2} + \frac{1}{2\sqrt{s_{i-1/2}}}\{X_s^{\mathrm{o}}\}_{i-1/2} + 2\sqrt{s_{i-1/2}}\,\{X_s^{\mathrm{o}}\}_{i-1/2} \quad \text{Eq 58}$$

where, again, the good analytical behaviour is kept. The radial derivatives are calculated, under the finite difference approximation up to first order, as

$$\{X_s^{\mathrm{e}}\}_{i-1/2} = \frac{\{\chi^{\mathrm{e,o}}\}_i - \{\chi^{\mathrm{e,o}}\}_{i-1}}{\Delta s} \quad \text{Eq 59}$$

This splitting is used for the calculation of the metrics terms, for example:

$$\{g_{\theta\theta}\}_{i-\frac{1}{2}} = \{R_\theta R_\theta + Z_\theta Z_\theta\}_{i-\frac{1}{2}} = \left\{\left[R_\theta^{\mathrm{e}} + \sqrt{s}R_\theta^{\mathrm{o}}\right]\left[R_\theta^{e} + \sqrt{s}R_\theta^{\mathrm{o}}\right] + \left[Z_\theta^{\mathrm{e}} + \sqrt{s}Z_\theta^{\mathrm{o}}\right]\left[Z_\theta^{\mathrm{e}} + \sqrt{s}Z_\theta^{\mathrm{o}}\right]\right\}_{i-\frac{1}{2}} =$$
$$\left\{R_\theta^{\mathrm{e}}R_\theta^{\mathrm{e}} + sR_\theta^{\mathrm{o}}R_\theta^{\mathrm{o}} + 2\sqrt{s}R_\theta^{\mathrm{e}}R_\theta^{\mathrm{o}} + Z_\theta^{\mathrm{e}}Z_\theta^{\mathrm{e}} + sZ_\theta^{\mathrm{o}}Z_\theta^{\mathrm{o}} + 2\sqrt{s}Z_\theta^{\mathrm{e}}Z_\theta^{\mathrm{o}}\right\}_{i-\frac{1}{2}} = \{R_\theta^{\mathrm{e}}R_\theta^{\mathrm{e}} + Z_\theta^{\mathrm{e}}Z_\theta^{\mathrm{e}} + sR_\theta^{\mathrm{o}}R_\theta^{\mathrm{o}} +$$
$$sZ_\theta^{\mathrm{o}}Z_\theta^{\mathrm{o}}\}_{i-1/2} + \sqrt{s_{1-1/2}}\{4R_\theta^{\mathrm{e}}R_\theta^{\mathrm{o}}\}_{i-1/2} \qquad \text{Eq 60}$$

where we can notice how some odd terms, when multiplied, become even.

B3. FLUX-SURFACE AVERAGE

The flux-surface average of a quantity X on the magnetic surface $S \equiv \partial V$ is obtained, in VMEC coordinates, as

$$\langle\langle X(s,\theta_v,\zeta_v)\rangle\rangle_{\partial V} = \frac{\int_{\partial V} X(s,\theta_v,\zeta_v)\frac{1}{|\nabla s|}\mathrm{d}S}{\int_{\partial V}\frac{1}{|\nabla s|}\mathrm{d}S} = \frac{\int_0^{2\pi}\int_0^{2\pi} X(s,\theta_v,\zeta_v)J_v\mathrm{d}\theta_v\mathrm{d}\zeta_v}{\int_0^{2\pi}\int_0^{2\pi} J_v d\theta_v\mathrm{d}\zeta_v} \qquad \text{Eq 61}$$

Similarly, in the case of Boozer coordinates,

$$\langle\langle \chi(s,\theta_{\mathrm{B}},\zeta_{\mathrm{B}})\rangle\rangle_{\partial V} = \frac{\int_0^{2\pi}\int_0^{2\pi}\chi(s,\theta_{\mathrm{B}},\zeta_{\mathrm{B}})J_{\mathrm{B}}\mathrm{d}\theta_B\mathrm{d}\zeta_{\mathrm{B}}}{\int_0^{2\pi}\int_0^{2\pi} J_{\mathrm{B}}\mathrm{d}\theta_{\mathrm{B}}\mathrm{d}\zeta_{\mathrm{B}}}. \qquad \text{Eq 62}$$

J_v and J_{B} are, respectively, the Jacobians of the change to VMEC and Boozer coordinates. The numerical implementation of this integral is effectuated on a regular grid of $[N_u \times N_w]$ points in real space, both in VMEC and BOOZ_XFORM. The grid points (θ_u, ζ_w) for the poloidal—toroidal domain are given by $\theta_u = 2\pi(w-1)/N_u$ and $\zeta_w = 2\pi(w-1)/N_w$ with $u \in [1, N_w]$. Then, the numerical approximation of the integral

$$\frac{1}{4\pi^2}\int_0^{2\pi}\int_0^{2\pi} f(\theta,\zeta)d\theta d\zeta \approx \frac{1}{N_u}\frac{1}{N_w}\sum_{u=1}^{N_u}\sum_{w=1}^{N_w} f(\theta_u,\zeta_w) \qquad \text{Eq 63}$$

shows spectral accuracy. Under the stellarator symmetry, VMEC integrates only half of the points, corresponding to the poloidal interval [0, π]. Then, the integral can be more efficiently calculated as

$$\frac{1}{N_u/2}\frac{1}{N_w}\left[\frac{1}{2}f(\theta_1,\zeta_w) + \frac{1}{2}f\left(\theta_{\mathrm{N_u}/2+1},\zeta_w\right) + \sum_{u=2}^{N_u/2}\sum_{w=1}^{N_w} f(\theta_u,\zeta_w)\right] \qquad \text{Eq 64}$$

choosing N_u and N_w as even numbers. The 1/2 coefficients are chosen to avoid duplicity when counting the nodes asociated with zero and π poloidal boundaries. A more compact expression is

$$\frac{1}{N_u/2}\frac{1}{N_w}\left[\sum_{w=1}^{N_w}\sum_{u=2}^{N_{u/2}}\alpha^u f(\theta_u,\zeta_w)\right] \qquad \text{Eq 65}$$

with

$$\alpha^u = \begin{cases}\frac{1}{2} \text{ if } u = 1, \frac{N_u}{2}+1 \\ 1 \text{ elsewhere}\end{cases} \qquad \text{Eq 66}$$

Then

$$\langle\langle X(s,\theta_{\mathrm{B}},\zeta_{\mathrm{B}})\rangle\rangle_{\partial V} \approx \frac{\sum_{u=2}^{N_u/2}\alpha^u X(s,\theta_u,\zeta_w) J_{\mathrm{B}}(s,\theta_u,\zeta_w)}{\sum_{u=2}^{N_u/2}\alpha^u\, J_{\mathrm{B}}(s,\theta_u,\zeta_w)}, \quad \text{Eq 67}$$

expression that will be used later.

B4. BOOZ_XFORM MODIFICATION

The metric elements can be calculated (either in VMEC or Boozer coordinates) as:

$$g_{ss} = R_s R_s + Z_s Z_s \quad \text{Eq 68}$$

$$g_{s\theta} = g_{\theta s} = R_s R_\theta + Z_s Z_\theta \quad \text{Eq 69}$$

$$g_{s\zeta} = g_{\zeta s} = R_s R_\zeta + Z_s Z_\zeta \quad \text{Eq 70}$$

$$g_{\theta\theta} = R_\theta R_\theta + Z_\theta Z_\theta \quad \text{Eq 71}$$

$$g_{\theta\zeta} = g_{\zeta\theta} = R_\theta R_\zeta + Z_\theta Z_\zeta \quad \text{Eq 72}$$

$$g_{\zeta\zeta} = R_\zeta R_\zeta + Z_\zeta Z_\zeta + R^2\zeta^2 \quad \text{Eq 73}$$

Most of the Boozer metric elements are ready in the BOOZ_XFORM library, except for g_{ss}. Here, based on the discretization previously described, we have implemented it as

$$\{g_{ss}\}_{i-1/2} = \left\{\left[R_s^{\mathrm{e}} + \frac{1}{2\sqrt{s}}R^{\mathrm{o}} + \sqrt{s}R_s^{\mathrm{o}}\right]^2 + \left[Z_s^{\mathrm{e}} + \frac{1}{2\sqrt{s}}Z^{\mathrm{o}} + \sqrt{s}Z_s^{\mathrm{o}}\right]^2\right\}_{i-1/2} = \left\{R_s^{\mathrm{e}}R_s^{\mathrm{e}} + sR_s^{\mathrm{o}}R_s^{\mathrm{o}} + \frac{1}{4s}R^{\mathrm{o}}R^{\mathrm{o}} + \frac{1}{\sqrt{s}}R_s^{\mathrm{e}}R^{\mathrm{o}} + 2\sqrt{s}R_s^{\mathrm{e}}R_s^{\mathrm{o}} + R^{\mathrm{o}}R_s^{\mathrm{o}} + Z_s^{\mathrm{e}}Z_s^{\mathrm{e}} + sZ_s^{\mathrm{o}}Z_s^{\mathrm{o}} + \frac{1}{4s}Z^{\mathrm{o}}Z^{\mathrm{o}} + \frac{1}{\sqrt{s}}Z_s^{\mathrm{e}}Z^{\mathrm{o}} + 2\sqrt{s}Z_s^{\mathrm{e}}Z_s^{\mathrm{o}} + Z^{\mathrm{o}}Z_s^{\mathrm{o}}\right\}_{i-1/2} = \left\{R_s^{\mathrm{e}}R_s^{\mathrm{e}} + Z_s^{\mathrm{e}}Z_s^{\mathrm{e}} + R^{\mathrm{o}}R_s^{\mathrm{o}} + Z^{\mathrm{o}}Z_s^{\mathrm{o}} + s(R_s^{\mathrm{o}}R_s^{\mathrm{o}} + Z_s^{\mathrm{o}}Z_s^{\mathrm{o}}) + \frac{1}{4s}(R^{\mathrm{o}}R^{\mathrm{o}} + Z^{\mathrm{o}}Z^{\mathrm{o}})\right\}_{i-1/2} + \frac{1}{\sqrt{s_{i-1/2}}}\{R_s^{\mathrm{e}}R^{\mathrm{o}} + Z_s^{\mathrm{e}}Z^{\mathrm{o}}\}_{1-1/2} + 2\sqrt{s_{i-1/2}}\,\{R_s^{\mathrm{e}}R_s^{\mathrm{o}} + Z_s^{\mathrm{e}}Z_s^{\mathrm{o}}\}_{i-1/2} \quad \text{Eq 74}$$

Now, notice that R and Z are defined on the *full* mesh (see Eq 49 and Eq 50) and the radial derivative of these expressions are defined on the *half* mesh (see Eq 59). Thus, the terms without derivatives on the full mesh has to be transformed to the *half* mesh using Eq 57. Therefore

$$\{g_{ss}\}_{i-1/2} = \{R_s^{\mathrm{e}}\}_{i-1/2}\{R_s^{\mathrm{e}}\}_{i-1/2} + \{Z_s^{\mathrm{e}}\}_{i-1/2} + \{Z\}_{i-1/2} + \langle R^{\mathrm{o}}\rangle_{i-1/2}\{R_s^{\mathrm{o}}\}_{i-1/2} + \langle R_s^{\mathrm{o}}\rangle_{i-1/2}\{R_s^{\mathrm{o}}\}_{i-1/2} + \mathrm{s}_{i-1/2}\left(\{R_s^{\mathrm{o}}\}_{i-1/2}\{R_s^{\mathrm{o}}\}_{i-1/2} + \{\mathrm{Z}_s^{\mathrm{o}}\}_{i-1/2}\{Z_s^{\mathrm{o}}\}_{i-1/2}\right) + \langle\frac{1}{4s}(R^{\mathrm{o}}R^{\mathrm{o}} + Z^{\mathrm{o}}Z^{\mathrm{o}})\rangle_{i-1/2} + \frac{1}{\sqrt{\mathrm{s}_{i-1/2}}}\left[\{R_s^{\mathrm{e}}\}_{i-1/2}\langle R_s^{\mathrm{o}}\rangle_{i-1/2} + \{Z_s^{\mathrm{e}}\}_{i-1/2}\langle Z_s^{\mathrm{o}}\rangle_{i-1/2}\right] + 2\sqrt{\mathrm{s}_{i-1/2}}\left[\{R_s^{\mathrm{e}}\}_{i-1/2}\{R_s^{\mathrm{o}}\}_{i-1/2} + \{Z_s^{\mathrm{e}}\}_{i-1/2}\{Z_s^{\mathrm{o}}\}_{i-1/2}\right] \quad \text{Eq 75}$$

Finally, after all the metric elements are available in Boozer coordinates, they are averaged out on the magnetic surfaces using Eq 67 and written on disk.

1135-9420